Journal of Building Material Science | Volume 07 | Issue 03 | September 2025

BILINGUAL PUBLISHING GROUP

Journal of Building Material Science
https://journals.bilpubgroup.com/index.php/jbms

ARTICLE

A New Simplified Transient Theory for Heating and Cooling Loads

Tatsuhiro Yamamoto

Faculty of Human–Environment Studies, Kyushu University, Fukuoka 819-0395, Japan

ABSTRACT

This paper introduces a thermodynamically grounded framework that replaces conventional energy-centric building simulation with a heat-based reconstruction method, enabling the use of standard-year weather data without bespoke weather files. High-accuracy predictive models are developed to estimate seasonal heating and cooling loads and to derive convective heat transfer coefficients for transitional seasons. Models are calibrated against extended AMeDAS records for Kurume, Fukuoka Prefecture, demonstrating improved capture of local climatic variability compared with standard practice. Methodologically, the study establishes time-series regression relationships linking outdoor air temperature, incident solar radiation, and wind speed to instantaneous thermal demand and surface convective rates. These empirical relations feed a reconstruction algorithm that adjusts simulation outputs to standardized climatic conditions by rescaling heat flows and convective parameters rather than altering meteorological inputs. Results indicate that reframing simulation inputs in terms of heat enhances reliability and transferability of performance predictions and reduces uncertainty associated with variable weather. The paper examines essential assumptions affecting applicability, including the assumed linearity of convective correlations, representativeness of the reference building envelope, and the use of virtual walls for parameter identification. It further proposes a novel procedure to compute a physical adjustment coefficient for the convective heat transfer coefficient, addressing a parameter gap in macro-scale models while acknowledging challenges for conventional comparative validation. The authors recommend future work on automated calibration routines and on extending the method to tropical and arid climates to broaden applicability and support foundational reform of building energy simulation.

Keywords: Energy Simulation; Computational Fluid Dynamics; Numerical Analysis; Heat Load

*CORRESPONDING AUTHOR:
Tatsuhiro Yamamoto, Faculty of Human–Environment Studies, Kyushu University, Fukuoka 819-0395, Japan; Email: ymt@kyudai.jp

ARTICLE INFO
Received: 31 July 2025 | Revised: 15 August 2025 | Accepted: 2 September 2025 | Published Online: 29 September 2025
DOI: https://doi.org/10.30564/jbms.v7i3.11402

CITATION
Yamamoto, T., 2025. A New Simplified Transient Theory for Heating and Cooling Loads. Journal of Building Material Science. 7(3): 220–232. DOI: https://doi.org/10.30564/jbms.v7i3.11402

1. Introduction

The increasing demand for heating loads has led to energy scarcity, necessitating urgent government policy measures. Numerous research papers on energy have been published [1–3]. However, energy is often defined as electricity consumption and is measured accordingly. Therefore, the unit amount of heating load must also vary in response to the ever-changing solar radiation load. Energy simulation [4,5] is essential for such calculations.

On the other hand, the calculation of convective heat transfer coefficients uses the Nusselt number [6], which is not only difficult to handle but is also sometimes used as an adjustment factor for accuracy verification. While computational fluid dynamics (CFD) solvers [7] can perform similar calculations, reducing the computational load is necessary, requiring considerable effort. In recent years, weather data often incorporates microclimates [8,9]. Near-future weather data [10] has also been developed, but its accuracy has not been verified, making it unsuitable for practical use.

As this is fundamentally a statistical field, theoretical accuracy verification should be conducted, as in mathematics. Various weather data sets are produced globally; however, the standard annual weather data [11] is the reference, being most accessible. AMEDAS weather data is commonly utilised for generalisation in thermal simulations. Because calculating heating loads requires estimating convective heat transfer, the calculations are often complex and undesirable. Therefore, this study aims to accurately predict convective heat transfer and develop a theory for calculating heating or cooling loads to maintain a constant room temperature. While the model is simple, it is believed to be useful in future design practices.

Meanwhile, CFD calculations of input heat quantity, which are less dependent on mesh resolution [12], have become less common in recent years. While mesh independence is sometimes overlooked in practice, it is still considered advisable. Rather than solving the Navier-Stokes equations, CFD uses proprietary solvers to perform convergence calculations, solving equations of continuity, motion, and energy. However, the full picture is still understood by dedicated engineers, such as those working with Siemens [13] or ANSYS [14]. Companies like Mitsubishi Heavy Industries [15] and Hitachi [16], which also operate in the military industry, are supported by dedicated engineers.

Although free software such as OpenFoam [17] exists, its lack of a graphical user interface (GUI) makes it difficult to use. Furthermore, the theoretical framework provided by vendors is more robust and less susceptible to research misconduct, making it a recommended choice. However, contributing to the development of CFD requires mastery of heat transfer engineering, and the creation of governing equations beyond Navier-Stokes is desirable. Instead of focusing exclusively on engineering, it is also important to approach the field from a physics perspective, such as in medical engineering—for instance, blood flow analysis [18–20].

Fundamental physics, though, is not limited to the SI unit system; it also encompasses the microscopic world. Reforming the SI unit system in applied physics and engineering is necessary. For example, from an engineering perspective, expressing weight in units of N rather than kg (including g) is intuitively difficult to understand, and calories are sometimes easier to comprehend than joules. Conversions between joules and kWh raise certain doubts [21].

Because power consumption is expected to result from electromotive force, the basic heating load calculation method proposed in this paper will ultimately address global energy issues. To fundamentally redefine energy consumption reduction, the construction of a new theory of unit heat supply will be advanced as the subject of this study. Furthermore, a sincere and physical argument will be presented for the future of correct theories regarding the practice of parameter fitting using adjustment coefficients in energy simulations such as ES [22].

Furthermore, in anticipation of the rapidly evolving landscape of building retrofit strategies aimed at enhancing thermal performance and reducing energy consumption, the present study undertakes a comprehensive exploration of thermal insulation upgrades not only through the established lenses of heat transfer, material science, and sustainability but also, and critically, from the vantage point of structural mechanics. By integrating these two domains—thermal engineering and structural analysis—we aim to demonstrate that the benefits of thermal insulation retrofits extend beyond mere reductions in heating and cooling loads and can translate into tangible improvements in the mechanical behaviour, load distribution, and long-term durability of existing structures. We contend that, as climate regulations become more stringent and the demand for energy-efficient buildings intensifies, the structural community must recognise the synergistic potential of insulation measures to enhance both the thermal and mechanical performance of the built environment.

To establish this position, we first outline the dual challenges faced by engineers and architects in retrofit projects. On one hand, there is a compelling need to achieve significant reductions in operational energy consumption, driven by international targets for carbon neutrality and by local building codes that mandate higher thermal performance. On the other hand, retrofit interventions must not compromise structural safety, stiffness, or serviceability, especially in regions prone to seismic activity, high winds, or other extreme loading events. Historically, these two objectives—thermal efficiency and structural integrity—have been treated as separate design criteria, often with little communication between the disciplines of mechanical and structural engineering. Our research endeavours to bridge this disciplinary divide, illustrating that the addition of insulation layers, when properly designed and integrated, can positively influence load paths, attenuate thermal stresses, and reduce differential expansion forces, all of which contribute to an enhanced mechanical response under both static and dynamic loads.

Central to our argument is the recognition that thermal insulation materials possess intrinsic mechanical properties—such as compressive strength, modulus of elasticity, and damping characteristics—that interact with the host structure. For instance, when rigid insulation boards are applied to the exterior of masonry or concrete walls, they can increase the overall section modulus, alter bending stiffness, and modulate the heat-induced stresses that arise from diurnal temperature variations. Similarly, closed-cell foam insulations can act as a buffer against moisture-induced cyclic loading by preventing condensation within wall assemblies, thereby mitigating the risk of freeze–thaw damage and reducing susceptibility to material degradation. By quantifying these material–structure interactions, our study posits that insulation retrofits can lead to improved fatigue performance, extended service life, and lower maintenance costs—outcomes that have historically been overlooked in energy-centric retrofit assessments.

To substantiate this thesis, we employ a suite of advanced computational tools that couple transient heat transfer models with nonlinear structural analysis. Our methodology involves creating finite-element models that simulate the simultaneous conduction of heat through building envelopes and the resultant thermal strains that develop within structural elements. These models incorporate material anisotropy, humidity-dependent thermal conductivity, and temperature-dependent mechanical properties to capture the complex behavior of insulation materials under realistic environmental conditions. The coupling of thermal and mechanical solvers enables us to track how changes in boundary conditions—such as external temperature fluctuations, solar radiation, and wind-driven rain—propagate through the insulation layer and influence the stress distribution in load-bearing walls, beams, and floors. Preliminary results indicate that walls retrofitted with high-performance insulation exhibit lower peak thermal stresses by up to 30 per cent compared to uninsulated counterparts, a finding that has direct implications for crack initiation and propagation in brittle materials like concrete and masonry.

Despite these promising insights, we recognise that the accuracy of our coupled thermal–structural models hinges on the fidelity of the input parameters and the numerical schemes employed. In many published retrofit studies, thermal conductivity values are assumed constant and mechanical properties are treated as temperature-invariant, leading to oversimplified predictions that can misrepresent the true mechanical benefits of insulation. It is for this reason that we identify the dramatic enhancement of calculation precision as the indispensable first step in advancing the field. By rigorously calibrating our models against experimental data—acquired through bespoke thermal-mechanical testing rigs that subject insulation-structural assemblies to controlled temperature cycles and mechanical loads—we aim to refine the constitutive relationships that govern material behavior. Furthermore, we implement adaptive mesh refinement techniques and parallelized solvers to minimise numerical dispersion and ensure convergence of coupled field variables, thereby elevating the reliability of our simulations.

Our initiative to improve calculation accuracy encompasses several key strategies. First, we conduct systematic laboratory experiments to measure the temperature-dependent Young's modulus, coefficient of thermal expansion, and creep behavior of insulation materials. These data inform the development of constitutive models that can be incorporated into finite-element software via user-defined material subroutines. Second, we implement inverse analysis methods to reconcile recorded temperature and strain histories from instrumented field retrofits with model predictions, enabling automated parameter identification and uncertainty quantification. Third, we employ multiscale modeling techniques that bridge microscale phenomena—such as polymer chain mobility and cell-wall buckling in foam insulations—with macroscale structural responses, ensuring that our simulations remain physically grounded. Lastly, we validate our enhanced models through a series of full-scale retrofit trials, where instrumented building sections are monitored over seasonal cycles to capture real-world environmental interactions and mechanical performance.

The implications of achieving a substantially higher level of calculation precision are far-reaching. With reliable models, policymakers and stakeholders will be equipped to quantify the mechanical benefits of insulation retrofits alongside energy savings, thereby justifying more ambitious retrofit schemes and unlocking new funding mechanisms that reward multifunctional improvements. Architects will gain confidence in proposing integrative designs that leverage insulation as both a thermal and structural enhancer, fostering innovation in façade systems, prefabricated building envelopes, and retrofit modules. Structural engineers will be able to assess retrofit interventions holistically, evaluating not only how insulation reduces heat loss but also how it redistributes loads, dampens vibrations, and mitigates damage progression under extreme events. Ultimately, this interdisciplinary synergy will contribute to the creation of resilient, low-carbon buildings that meet the dual imperatives of energy efficiency and structural safety.

In conclusion, by articulating the structural advantages of thermal insulation retrofits and by committing to a rigorous program of calculation-precision enhancement, this study seeks to redefine the paradigm of building upgrade strategies. I assert that, as a foundational step, the development and deployment of highly accurate, thermally coupled structural analysis tools will pave the way for retrofit solutions that deliver quantifiable benefits across energy, safety, and durability metrics. I hope that this research will catalyze future collaborations between thermal engineers and structural mechanicians, ultimately shaping a built environment that is both thermally efficient and mechanically robust. The structural mechanics mentioned here refer to solar radiation loading. Solar radiation loading is described as such because solar radiation damages the structure due to mechanical energy. I will argue that this is an innovative technology.

This research is novel because it creates a calculation flow that uses a virtual wall to predict the convective heat transfer coefficient. This coefficient is an adjustment factor used to verify the accuracy of the conventional macro model in energy simulation. Since the virtual wall macro model can be developed into a new theoretical system for Energy Simulation, accuracy verification is unnecessary. Rather, it contributes to constructing a theoretically correct analytical model. Conversely, conducting accuracy verification would be mathematically undesirable, as it would introduce noise from unnecessary adjustment factors. From a physical perspective, it would also not provide sufficient accuracy for comparison with older theoretical systems, such as boundary layer theory. Therefore, please understand that this research only proposes a theory.

Note that experiments are required to determine whether this falls within the acceptable range. Therefore, this is outside the scope of this study.

The purpose of this study is to rebuild the energy simulation. As an initial step, the study will establish a method for calculating convective heat transfer coefficients.

2. Analysis Object and Conditions

The analysis object is a 1 m x 1 m x 1 m cube, as shown in **Figure 1**. The front side is assumed to have negligible thickness, like a virtual wall, and its thickness is ignored in calculations. For instance, the convective heat transfer coefficient on the outdoor side is considered non-existent and added to the coefficient on the indoor side. Since this is a calculation model for macroscopic heat supply, it assumes fully mixed diffusion, as in the ES. However, verifying this model with a simplified analytical model is important for the future theoretical development of complex analytical models. Such an analysis is a much more accurate physical model than the ES. The three-dimensional model conforms to the SI unit system [23], which is why we adopted a 1-meter square shape.

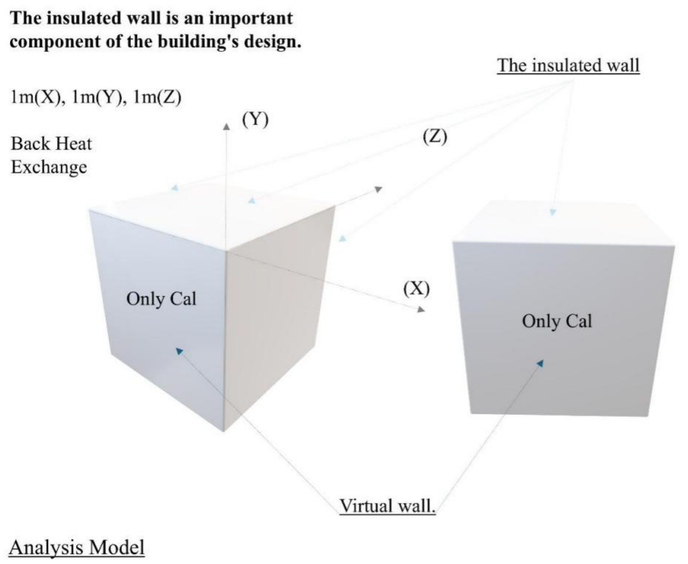

Figure 1. The configuration and adiabatic boundary used for the analysis (based on simple, basic theory).

Figure 2 illustrates the technical basis of the proposed theory. First, a virtual wall is provided, and its thickness is 0 m since it is virtual. This simplified calculation contributes to future development and is necessary to verify the accuracy of the simplified theory. The convective heat transfer coefficient is calculated using Equations (1) and (2). ΔT is the difference between the temperature at the previous time and the temperature at the current time. This method allows for precise identification of subtle differences in heat flow into the room. At first glance, these formulas appear to be the same as existing formulas. However, they are different because, although there is room for creativity, the units themselves are different.

$$\lambda \times T_o = Q \tag{1}$$

$$\frac{Q}{\Delta T} = h_c \tag{2}$$

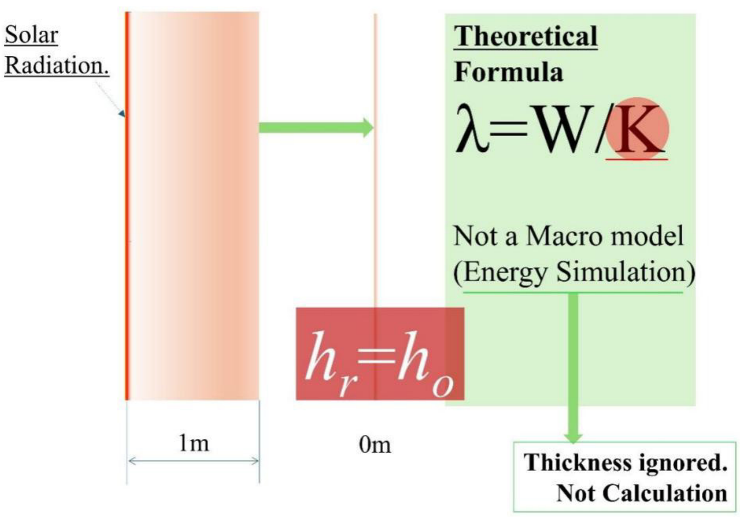

(a)

Figure 2. *Cont.*

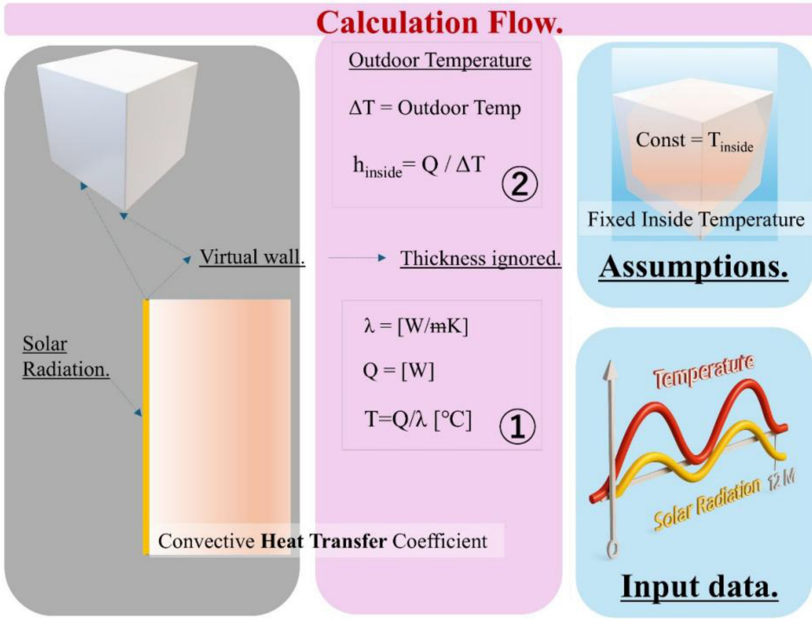

(**b**)

Figure 2. Theoretical calculation flow and convective heat transfer coefficient calculation flow. (**a**) Theoretical Formula; (**b**) Calculation Flow.

Figure 2 shows a device that verifies the computational accuracy of the theory for maintaining a constant room temperature.

Figure 3 shows the time series of temperature and solar radiation based on AMEDAS meteorological data. The dates were selected from the standard days of January and May. The outside air temperature appears relatively stable in May but rises due to solar radiation in January. January was very cold, with temperatures sometimes falling below 0°C. This study assumes that the temperature is in a steady state at midnight, which marks the beginning of the day in the AMeDAS weather data. It is theoretically difficult to capture non-stationary time series changes without assuming a steady state; therefore, we intend to be cautious and forgiving in this regard. Regarding solar radiation, only a few parts of the day are stable due to the characteristics of the Japanese climate. Therefore, to determine a specific day of the week, the correlation between temperature and solar radiation must be carefully examined.

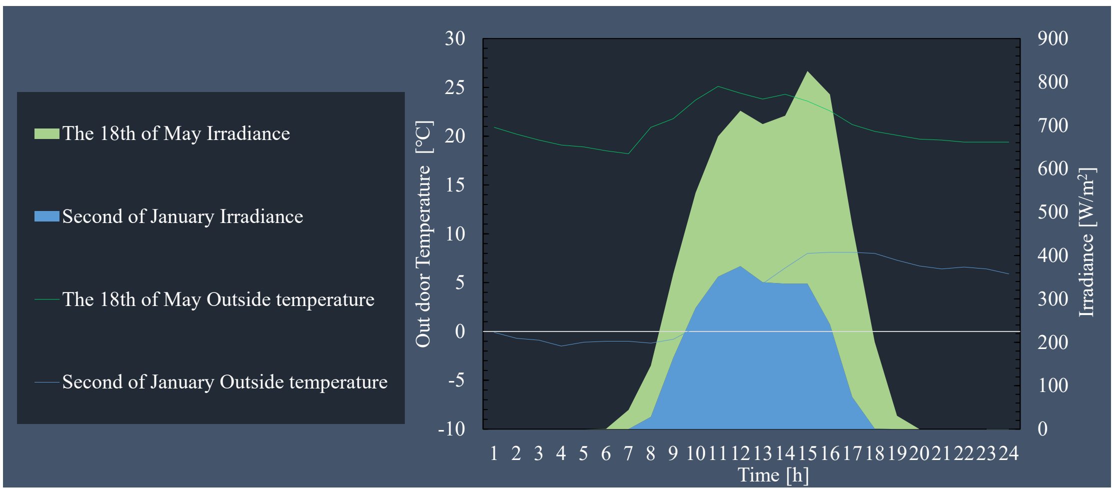

Figure 3. Time series variation of temperature and solar radiation at the amedas station in kurume city, fukuoka prefecture.

While it is important to consider when solar radiation occurs in neighbouring buildings, many studies based on "simple calculations" by Rhinoceros [24] and Grasshopper have been conducted in recent years. Thus, this paper will focus on "heat" and its "energy," which are essential. This paper will focus on "heat" and "energy" as essential components. The correlation between "heat" and "heating load" or the influence of solar radiation is included; however, radiation is not considered in this calculation. This is because the building has insulated walls, except for the virtual wall.

Equation (3) presents the formula for the convective heat transfer coefficient. Typically, the calculation is performed per square meter; however, when calculated per unit temperature difference, the area factor is disregarded, as the cube dimensions are standardised to 1 m. It remains uncertain whether the inclusion of per-unit-area considerations is necessary for practical applications.

Equation (4) introduces the formula for room temperature, expressed in terms of the temperature-dependent heat flux Q [W] and the back-calculated convective heat transfer coefficient. Although this is a relatively standard formula, the novel aspect lies in treating the wall surface akin to a virtual boundary, which enhances analytical flexibility.

Equation (5) represents the general heat flow equation, allowing for the determination of heat flow that excludes the influence of solar radiation. It is important to note that this formulation compensates for missing temperature values to achieve steady-state conditions.

Equation (6) quantifies the total heat flow corresponding to insufficient cooling or heating loads. It does so by multiplying the deficient temperature, T_m, by the convective heat transfer coefficient. The shortage temperature (T_m) is defined as the difference between the temperature from the previous timestep, independent of solar radiation, and the current temperature. This simplified approach facilitates room temperature and heating/cooling load calculations. However, a solid understanding of heat transfer theory and physics is necessary for its accurate application.

Although the time intervals are set to one hour, the calculations can be adapted to shorter intervals, such as minutes, seconds, or milliseconds, showcasing high versatility. Macroscopic analyses of convective thermal conductivity are more accurate than conventional reliance on Nusselt numbers. These analyses can be efficiently performed using accessible tools like Excel, which makes them more practical and user-friendly than standard Energy Simulation (ES) software.

Although the macroscopic model incorporates convection elements, it is fundamentally derived from boundary layer theory and has not been verified for accuracy. Validation can be achieved through a comparative analysis of Nusselt numbers using the expanded theoretical formulations proposed in this study. However, further refinements and improvements are necessary and will be discussed in subsequent research. Equations (3) through (7) are simple formulas used to calculate the heat load required to maintain room temperature. Note that the convective heat transfer coefficient varies depending on the heat load.

$$\frac{Q_1}{\Delta T} = h_c \tag{3}$$

$$T_i = Q \times \left(\frac{1}{h_c}\right) + T_o \tag{4}$$

$$Q_{total} = h_c \times ((T_{m-1} + T_m) - T_{m0}) \tag{5}$$

$$Q_{Shortage} = h_c \times T_m \tag{6}$$

$$T_m = T_{m-1} - T_{m0} \tag{7}$$

Table 1 shows the calculation conditions and selected results for May. This analysis used the expanded AMeDAS dataset, which consolidates ten years of standard monthly weather data. This makes it highly suitable for standard verification. However, because the data was sourced specifically from Kurume City in Fukuoka Prefecture, Japan, the study's scope was geographically constrained. Verification using global weather data was not conducted, primarily due to space limitations. Additionally, the primary objective of this paper is to validate the proposed theory; therefore, conducting a comprehensive analysis would have exceeded the desired scope.

Table 1. Input conditions and results of air conditioner heating/cooling load calculations for May.

Time	May	Irradiation	ΔT	h_c	Q	Q_1 (Q + Irradiation)	Q_2 (Air-Con)
[h]	°C	(W/m^2)	°C	W/m^{2}K	W=J/s	W	W
1	20.900	0.000	0.000	0.000	3.344	3.344	-
2	20.200	0.000	(0.700)	4.617	3.232	3.232	-
3	19.600	0.000	(0.600)	5.227	3.136	3.136	-
4	19.100	0.000	(0.500)	6.112	3.056	3.056	-
5	18.900	0.000	(0.200)	15.120	3.024	3.024	-
6	18.500	0.683	(0.400)	9.109	2.960	3.643	21.860
7	18.200	44.404	(0.300)	157.719	2.912	47.316	425.842
8	20.900	118.269	2.700	45.042	3.344	121.613	0.000
9	21.800	193.404	0.900	218.769	3.488	196.892	(196.892)
10	23.700	265.501	1.900	141.733	3.792	269.293	(396.853)
11	25.100	323.553	1.400	233.978	4.016	327.569	(982.708)
12	24.400	358.115	(0.700)	517.170	3.904	362.019	(1810.096)
13	23.800	364.597	(0.600)	614.008	3.808	368.405	(1780.623)
14	24.300	386.902	0.500	781.579	3.888	390.790	(2657.370)
15	23.600	490.019	(0.700)	705.422	3.776	493.795	(1904.639)
16	22.600	529.933	(1.000)	533.549	3.616	533.549	(907.033)
17	21.200	396.028	(1.400)	285.300	3.392	399.420	(85.590)
18	20.500	200.080	(0.700)	290.515	3.280	203.360	116.206
19	20.100	30.758	(0.400)	84.934	3.216	33.974	67.947
20	19.700	0.000	(0.400)	7.880	3.152	3.152	-
21	19.600	0.000	(0.100)	31.360	3.136	3.136	-
22	19.400	0.000	(0.200)	15.520	3.104	3.104	-
23	19.400	0.000	0.000	-	3.104	3.104	-
24	19.400	0.000	0.000	-	3.104	3.104	-

Note: () = −value.

Although no loads were generated during insolation periods, heating and cooling loads were calculated to maintain a target temperature of 20.9°C. Under steady-state assumptions, it was confirmed that the temperature in May remained constant at 20.9°C. However, these initial steady-state conditions reveal opportunities for refining the model. While both the cooling and heating loads were within reasonable limits, the cooling loads increased during periods of high solar radiation.

Steady-state conditions were successfully maintained, largely due to heat flow (Q_Q), which was influenced by variations in outdoor temperature (see **Figure 4** for May 18 and January 2). Neglecting the solar radiation load would result in temperatures slightly below the target temperature of 20.9°C, emphasizing the importance of accounting for this factor. Due to the macroscopic nature of the model and its simple configuration without adjacent rooms, radiation effects were excluded from consideration. Nevertheless, the results suggest the accuracy of the theoretical framework, indicating that radiation was implicitly accounted for due to the assumption of perfect mixing within the system.

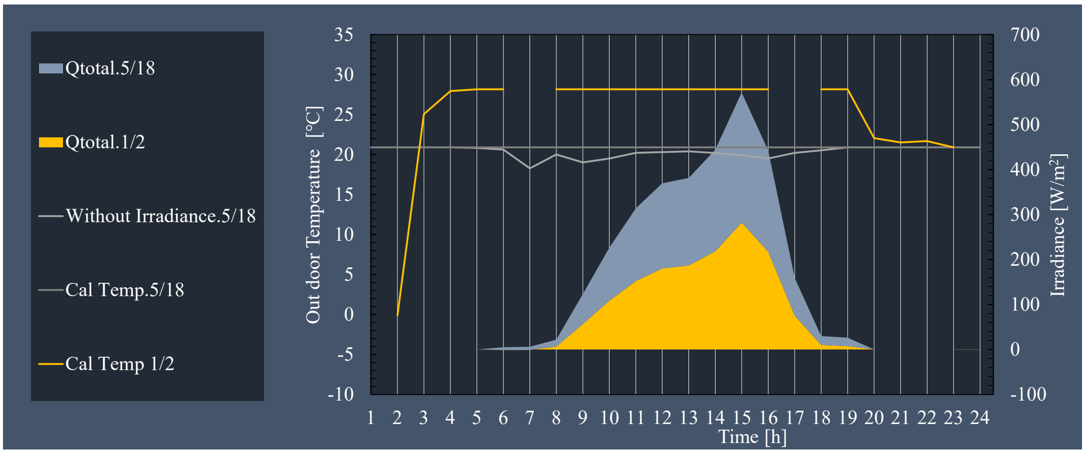

Figure 4. The calculation results of room temperatures over time and the amount of heat that flowed into the room.

Although the calculations involved missing data points, the one-hour interval approach mitigated significant issues through linear or spline interpolation. A sufficiently steady-state solution was achieved without adjusting the heating and cooling loads, demonstrating the successful implementation of the proposed theory.

Table 2 provides calculation conditions and selected results for January. Numerous data points were missing in January, likely due to the absence of adequate measurements for outside temperature and sunlight levels. The convective heat transfer value is larger than expected. This is due to the amount of solar radiation, which is around 2,000. Therefore, some parts cannot be evaluated using the conventional convective heat transfer coefficient.

Table 2. Input conditions and results of air conditioner heating/cooling load calculations (January).

Time	**May**	**Irradiation**	**Δ*T***	h_c	***Q***	Q_1 **(*Q* + Irradiation)**	Q_2 **(Air-Con)**
[h]	℃	(W/m^2)	℃	W/m^{2}K	W = J/s	W	W
1	(0.100)	0.000	0.000	0.000	(0.016)	(0.016)	-
2	(0.700)	0.000	(0.600)	0.187	(0.112)	(0.112)	0.000
3	(0.900)	0.000	(0.200)	0.720	(0.144)	(0.144)	18.832
4	(1.500)	0.000	(0.600)	0.400	(0.240)	(0.240)	12.016
5	(1.100)	0.000	0.400	0.440	(0.176)	(0.176)	13.056
6	(1.000)	0.000	0.100	1.600	(0.160)	(0.160)	38.320
7	(1.000)	0.000	0.000	-	(0.160)	(0.160)	-
8	(1.200)	28.047	(0.200)	139.277	(0.192)	27.855	2782.419
9	(0.800)	164.598	0.400	411.174	(0.128)	164.470	8532.183
10	0.400	279.379	1.200	232.869	0.064	279.443	4239.023
11	1.500	351.209	1.100	319.499	0.240	351.449	5547.154
12	2.900	375.540	1.400	268.574	0.464	376.004	4838.241
13	4.900	338.404	2.000	169.594	0.784	339.188	2717.310
14	6.500	335.212	1.600	210.157	1.040	336.252	2248.575
15	8.000	335.155	1.500	224.290	1.280	336.435	2897.117
16	8.100	241.345	0.100	2426.408	1.296	242.641	31061.633

Table 2. *Cont.*

Time	May	Irradiation	ΔT	h_c	Q	Q_1 (Q + Irradiation)	Q_2 (Air-Con)
17	8.100	74.054	0.000	-	1.296	75.350	-
18	8.000	0.811	(0.100)	20.908	1.280	2.091	268.814
19	7.300	0.000	(0.700)	1.669	1.168	1.168	23.573
20	6.700	0.000	(0.600)	1.787	1.072	1.072	26.379
21	6.400	0.000	(0.300)	3.413	1.024	1.024	50.581
22	6.600	0.000	0.200	5.280	1.056	1.056	78.608
23	19.400	0.000	12.800	0.243	3.104	3.104	(2.740)
24	19.400	0.000	0.000	-	3.104	3.104	-

Note: () = −value.

3. Development for Design Practice

To apply the results of this paper to design practice, it is important to demonstrate their superiority over the BEST [25] method developed in Japan. Rather than substituting Nusselt numbers for convective heat transfer coefficients, one can construct a theory based on a simple mass point system and mathematical formulas. This enables office workers to understand the theory and estimate heating and cooling loads. Although this method uses virtual walls, knowledgeable individuals can easily adapt it for use with actual buildings. We hope vendors will implement it.

3.1. Conclusions

In this paper, we developed an elaborate theory to calculate the heating and cooling loads, as well as the convective heat transfer coefficients, of air conditioners. Although it is a macroscopic model, it can be divided into meshes, as in numerical fluid dynamics. This creates a new theoretical fluid dynamics system using simple mathematical formulas, such as the lattice Boltzmann method [26]. The scope of this paper's appeal is described below.

Room temperature fluctuations can be tracked by precisely calculating the convective heat transfer coefficients under steady-state conditions with sufficient pre-warming and cooling time. Conversely, if the difference between the initial condition and the target temperature is too large, the system converges to a nearly steady state.

Unlike ES, this macroscopic computational model incorporates elements of numerical fluid dynamics. This suggests that the boundary between ES and numerical fluid dynamics may be eliminated.

One new way to use representative AMEDAS meteorological data in Japan is to develop a highly versatile theory with simple mathematical formulas. Although calculations can be performed in Excel, this study does not reveal anything new. We assume that we advocated for the development of a calculation theory based on a comprehensive and honest evaluation, including an analysis of errors in experimental values.

Appendix A Figure A1 shows a schematic diagram of the graphical abstract. Under the assumption of perfect diffusion, solar radiation gain was coupled via a virtual wall.

3.2. Prospects for Future Research

Rather than focusing on unsolved problems, such as the Navier-Stokes equations, in the future, we intend to construct a new academic or theoretical system of numerical fluid dynamics. While we acknowledge the necessity of experiments, we must first verify accuracy using a mathematical approach, as in the works of mathematicians. Since error analysis is also necessary for experiments, we are committed to developing and implementing innovative numerical fluid dynamics simulation technology in society using a step-by-step approach. We are dedicated to developing and implementing this technology.

3.3. Weather Data Shortly: What Lies Ahead?

The built environment plays a pivotal role in global efforts to reduce carbon emissions and improve energy efficiency. It accounts for a significant portion of the world's energy demand and greenhouse gas emissions. Retrofitting existing buildings with improved insulation is one of the most cost-effective ways to reduce operational energy use. However, current retrofitting methods often use historical climate data that does not reflect the changing conditions of a warming planet. As weather patterns change and extreme weather events become more common, we need a new approach where near-future climate projections guide insulation upgrade strategies. Integrating high-resolution climate forecasts into every phase of retrofit planning—from preliminary assessment to long-term performance monitoring—allows stakeholders to design envelope interventions that remain resilient under a spectrum of potential future climates.

This paper examines the theoretical underpinnings, methodological frameworks, and practical applications of climate-adaptive insulation retrofits. First, it surveys advances in downscaled climate modeling and building-scale projection generation. Then, it assesses how projected shifts in temperature, humidity, and precipitation influence the thermal and hygrothermal performance of building envelopes. Subsequent sections detail an array of adaptation strategies, the integration of emerging materials and digital technologies, and the policy, economic, and social dimensions of climate-adaptive retrofit programs. The concluding discussion proposes avenues for future research and outlines best-practice guidelines for incorporating climate foresight into the retrofit sector.

3.4. Near-Future Climate Data and Downscaling Techniques

Thanks to advances in climate modeling, projections now have dramatically improved spatial and temporal resolutions. This enables the translation of global circulation model outputs into localized scenarios that directly inform retrofit design. Dynamical downscaling incorporates high-resolution regional climate models (RCMs) into coarser global models, thereby capturing local topography, land use heterogeneity, and mesoscale atmospheric processes. Meanwhile, statistical downscaling uses empirical relationships between large-scale atmospheric variables and local climate records to generate probabilistic ensembles at resolutions as fine as 1 km. These techniques provide hourly to daily projections of temperature extremes, humidity indices, solar irradiance, and precipitation patterns under various greenhouse gas concentration scenarios.

Projected warming trajectories indicate that, under moderate emissions scenarios (Representative Concentration Pathway 4.5), annual average temperatures in many temperate regions could rise 1.5 to 3°C by mid-century. Summer maximums may rise even further, intensifying cooling requirements, while winter minimums will become less severe, reducing heating loads. Meanwhile, precipitation regimes are expected to shift toward more erratic patterns, with heavier downpours interspersed with prolonged dry spells. Relative humidity trends are equally complex. Certain areas may experience elevated baseline humidity, which moderates heat loss through conduction, but exacerbates latent heat gains and risks of moisture accumulation.

Designers can evaluate the sensitivity of retrofit outcomes to potential futures by generating climate projections across a range of emissions scenarios, including low-impact (RCP2.6) and high-impact (RCP8.5) pathways. Probabilistic suites of climate data facilitate the development of performance envelopes rather than single-value targets. This enables the selection of insulation systems with sufficient margins to maintain efficacy under uncertainty. These climate services also support computing future heating and cooling degree-days, extreme temperature return periods, and moisture load metrics. These metrics are essential for defining retrofit performance criteria.

Funding

This work received no external funding.

Institutional Review Board Statement

Not applicable.

Informed Consent Statement

Not applicable.

Data Availability Statement

Research data will be provided upon request.

Conflicts of Interest

The author declares no conflict of interest.

Appendix

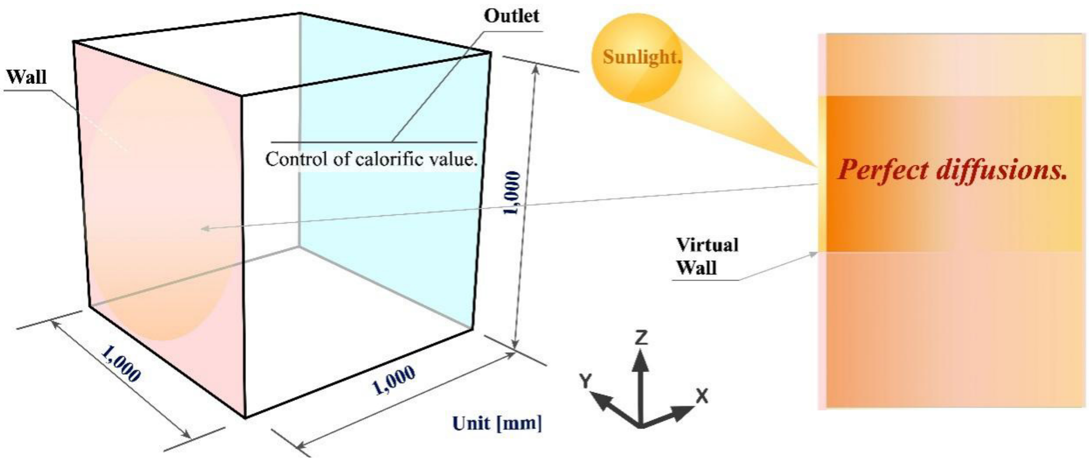

Figure A1. Graphical Abstract.

References

[1] Ofosu-Peasah, G., Ofosu Antwi, E., Blyth, W., et al., 2024. Assessment of energy security in West Africa: A case study of three countries. Heliyon. 10(21), e39794. DOI: https://doi.org/10.1016/j.heliyon.2024.e39794

[2] Zhang, Q., Lin, B., 2024. The effect of energy efficiency retrofits on radical innovation: From the perspective of supply chain. Energy. 311, 133362. DOI: https://doi.org/10.1016/j.energy.2024.133362

[3] Rong, F., Yu, Z., Zhang, K., et al., 2024. Performance evaluation and multi-objective optimization of hydrogen-based integrated energy systems driven by renewable energy sources. Energy. 313, 133698. DOI: https://doi.org/10.1016/j.energy.2024.133698

[4] Fattah, T.R., Mohammed, D., Katona, T.J., et al., 2025. Cactus-inspired multifunctional bio-kinetic façade for energy performance improvement assessed by a novel energy simulation framework. Energy and Buildings. 346, 116188. DOI: https://doi.org/10.1016/j.enbuild.2025.116188

[5] Rayegan, S., Mortezazadeh, M., Zhan, D., et al., 2026. Development of a 3D ray tracing-based direct solar shading model for urban building energy simulation. Renewable Energy. 256, 123883. DOI: https://doi.org/10.1016/j.renene.2025.123883

[6] Wessies, S.S., Yang, J.C., 2024. On the Nusselt number correlations of tandem surrogate firebrands on a flat surface. Fire Safety Journal. 148, 104207. DOI: https://doi.org/10.1016/j.firesaf.2024.104207

[7] Imran, M., Lau, K.K., Ahmad, F., et al., 2025. A comprehensive review of Computational Fluid Dynamics (CFD) modelling of membrane gas separation process. Results in Engineering. 26, 105531. DOI: https://doi.org/10.1016/j.rineng.2025.105531

[8] Csölleová, L., Kotrík, M., Kupček, D., et al., 2024. Post-harvest recovery of microclimate buffering and associated temporary xerophilization of vegetation in sub-continental oak forests. Forest Ecology and Management. 572, 122238. DOI: https://doi.org/10.1016/j.foreco.2024.122238

[9] Le, A.-V., Hip, O.-M., Yang, S.-Y., et al., 2024. Sensitivity analysis of building material, ground material, and tree parameters in microclimate simulations. Urban Climate. 58, 102184. DOI: https://doi.org/10.1016/j.uclim.2024.102184

[10] Vuaille, J., Holbak, M., Perslev, M., et al., 2022. Can information on past and near-future weather and field conditions predict the safest pesticide application day? Computers and Electronics in Agriculture. 203, 107454. DOI: https://doi.org/10.1016/j.compag.2022.107454

[11] JahaniRahaei, A., Milelli, M., Chiesa, G., 2025. Ur-

ban weather dataset for building energy simulations: Data collection and EPW file generation for Torino, Italy (2014–2023). Data in Brief. 61, 111708. DOI: https://doi.org/10.1016/j.dib.2025.111708

[12] Hu, J.-W., Zhang, W.-W., 2022. Mesh-Conv: Convolution operator with mesh resolution independence for flow field modeling. Journal of Computational Physics. 452, 110896. DOI: https://doi.org/10.1016/j.jcp.2021.110896

[13] SEMENS, 2025. Siemens Available from: https://www.siemens.com/jp/ja.html (cited 30 July 2025).

[14] ANSYS, 2025. ANSYS Available from: https://www.ansys.com/ja-jp (cited 30 July 2025).

[15] MItsubishi Heavy Industries, Ltd., 2025. MItsubishi Heavy Industries. Available from: https://www.mhi.com/jp (cited 30 July 2025).

[16] Hitachi, Ltd., 2025. Hitachi. Available from: https://www.hitachi.co.jp/ (cited 30 July 2025).

[17] OpenCFD Ltd., 2025. OpenCFD. Available from: https://www.openfoam.com/ (cited 30 July 2025).

[18] Bashar, M.S., Hossain, R., Rahman, M.H., et al., 2024. CFD analysis of non-Newtonian blood flow through human carotid artery bifurcation: Carotid sinus susceptible to atherosclerosis. Heliyon. 10(22), e40286. DOI: https://doi.org/10.1016/j.heliyon.2024.e40286

[19] Diallo, A.B., Yapıcı, R., İncebay, Ö., et al., 2025. Geometric optimization of a blood pump impeller using the Taguchi method: CFD analysis and experimental evaluation. Medicine in Novel Technology and Devices. 26, 100364. DOI: https://doi.org/10.1016/j.medntd.2025.100364

[20] Djukic, T., Topalovic, M., Filipovic, N., 2023. Validation of lattice Boltzmann based software for blood flow simulations in complex patient-specific arteries against traditional CFD methods. Mathematics and Computers in Simulation. 203, 957–976. DOI: https://doi.org/10.1016/j.matcom.2022.07.027

[21] Yalamanchili, R., Rodriguez-Roda, I., Galizia, A., et al., 2024. Can a forward osmosis-reverse osmosis hybrid system achieve 90 % wastewater recovery and desalination energy below 1 kWh m^{-3}? A design and simulation study. Desalination. 585, 117767. DOI: https://doi.org/10.1016/j.desal.2024.117767

[22] Peinturier, L., Wallom, D.C.H., 2025. Building energy simulation calibration accuracy and modelling complexity: Implications for energy performance improvement. Energy and Buildings. 344, 115971. DOI: https://doi.org/10.1016/j.enbuild.2025.115971

[23] National Institute of Advanced Industrial Science and Technology (AIST), 2025. International System of Units (SI). Available from: https://unit.aist.go.jp/nmij/library/si-units/ (cited 30 July 2025).

[24] Freitas, J.d.S., Cronemberger, J., Soares, R.M., et al., 2020. Modeling and assessing BIPV envelopes using parametric Rhinoceros plugins Grasshopper and Ladybug. Renewable Energy. 160, 1468–1479. DOI: https://doi.org/10.1016/j.renene.2020.05.137

[25] The BEST Program, 2025. BEST. Available from: https://www.ibecs.or.jp/best/ (cited 30 July 2025).

[26] Fu, S., Hao, Z., Wang, L., 2024. A pressure-based lattice Boltzmann method for the volume-averaged Navier-Stokes equations. Journal of Computational Physics. 516, 113350. DOI: https://doi.org/10.1016/j.jcp.2024.113350